

Stability Analysis of an Axisymmetric Boundary Layer

N. Vinod, Hamsa Balakrishnan[†] & Rama Govindarajan

(Fluid Dynamics Unit, Jawaharlal Nehru Centre for Advanced Scientific Research)
Bangalore- 560064, INDIA

([†] presently at Stanford University, CA 94305, USA)

ABSTRACT: A linear stability analysis of the boundary layer over an axisymmetric body shows that transverse curvature has a significant effect on the stability. Depending on the curvature axisymmetric or non-axisymmetric modes may be dominant. Detailed computations of energy balance are also done. The disturbance kinetic energy production indicates that several modes can co-exist giving rise to possibilities for different routes to transition.

Introduction

The destabilization of the laminar boundary layer is the first step in the process of transition to turbulence. A range of analytical and experimental work has been done to understand the stability of 2D-laminar boundary layer, but we are interested here in the boundary layer over an axisymmetric body. In the case of 2D mean flow one usually resorts to the Squire's theorem, which states that for every 3D disturbance, there exist a corresponding 2D disturbance which is destabilised at a lower Reynolds number. This theorem however not apply to axisymmetric flows and here an assortment of 3D modes may go unstable first. Although the behavior of non-axisymmetric modes in pipe flows has been studied both theoretically (Lessen, Sadler & Liu, 1968) and experimentally (Leite, 1959 and Fox, Lessen & Bhat, 1968), investigations on external boundary layers on axisymmetric bodies are sparse in the literature. An exception is the work by Rao (1967) about the effect of transverse curvature on the transition in the flow around an axisymmetric body. He found that transverse convex curvature has a destabilising effect on the laminar flow boundary layer subjected to small disturbances. This equations and analysis had many limitations due to the absence of computing facilities at that time.

It is therefore our aim here to study the stability of boundary layers on axisymmetric bodies (such as underwater bodies), moving parallel to their axis. Our analysis is limited in this abstract to thick cylinders, i.e., those whose radius is much higher than the thickness of the boundary layer; results on general bodies will be presented at the conference. We also neglect the spatial development of the boundary layer. We find that modes $n=0,1$ or 2 may dominate depending on the body radius and the Reynolds number, where n is the number of waves encircling the body. From computations of energy balance of the disturbance kinetic energy we find that these modes can co-exist simultaneously, i.e. their production layers coincide which would promote non-linear interactions at an early stage and lead to a different kind of transition.

Formulation of the stability equations

Equations of the linear stability of this flow are obtained by the standard procedure. We begin with the Navier-Stokes and continuity equations in polar cylindrical coordinates. They are non-dimensionalised using the free-stream velocity, V and the momentum thickness θ , as the velocity and length scales respectively. The Navier-Sokes equations are written as,

$$\frac{\partial U}{\partial t} + U \cdot \nabla U = \nabla p + \frac{1}{\text{Re}} \nabla^2 U \quad (1)$$

where R_e is the Reynolds number,

$$R_e = \frac{V\theta}{\nu} \quad (2)$$

ν is the kinematic viscosity. The basic flow is assumed to be parallel and the components of the mean flow velocity in the radial and azimuthal directions are zero. Here the U is the local stream velocity which is defined as,

$$\vec{U} = v_z \vec{z} + v_r \vec{r} + v_\theta \vec{\theta} \quad (3)$$

All flow quantities are split into their respective mean and a fluctuating part, where the suffixes, z , r and θ denote the streamwise, radial and azimuthal components respectively. The equations are linearised by neglecting the higher order terms in the disturbance. The disturbance is taken to be in

$$v_z = U + \hat{v}_z; \quad v_r = \hat{v}_r; \quad v_\theta = \hat{v}_\theta \quad p = P + \hat{p} \quad (4)$$

normal mode form:

$$\hat{\psi} = \frac{1}{2} (\psi(r) \cdot \exp[i\{\alpha(x - ct) + n\theta\}] \cdot \exp(\omega_i t) + c.c.), \quad (5.a)$$

$$\hat{\phi} = \frac{1}{2} (\phi(r) \cdot \exp[i\{\alpha(x - ct) + n\theta\}] \cdot \exp(\omega_i t) + c.c.), \quad (5.b)$$

such that,

$$\hat{v}_z = \frac{1}{r} \frac{\partial \hat{\psi}}{\partial r}; \quad \hat{v}_r = -\frac{1}{r} \left(\frac{\partial \hat{\psi}}{\partial z} + \frac{\partial \hat{\phi}}{\partial \theta} \right) \quad \text{and} \quad \hat{v}_\theta = \frac{\partial \hat{\phi}}{\partial r}. \quad (6)$$

Here we have made use of the equation of continuity to define ψ and ϕ , reducing the number of equations from 4 to 3. α is the streamwise wave number, c is the phase speed and ω_i is the growth rate of the disturbance. n is an integer which is the number of waves encircling the body. When $n=0$ the disturbance is axisymmetric, non-zero values represent non-axisymmetric disturbances. Making use of equations 4 and 5 and eliminating the pressure term, we arrive at two equations of 4th order, which are,

$$\begin{aligned} (U - c) \left[\psi'' - \frac{\psi'}{r} - \alpha^2 \psi \right] - (U'' - \frac{U'}{r}) \psi - (U - c) \alpha n \phi - \frac{n}{\alpha} (U'' \phi + \phi' U' - \frac{\phi}{r} U') \\ = \frac{1}{i\alpha R_e} \left[\psi^{iv} - \frac{2}{r} \psi''' + \frac{3}{r^2} \psi'' - 2\alpha^2 \left(\psi'' - \frac{\psi'}{r} \right) + \alpha^4 \psi \right. \\ \left. - \frac{n^2}{r^2} \left(\psi'' - \frac{3}{r} \psi' - \alpha^2 \psi \right) - \frac{3}{r^3} \psi' - n\alpha \left[\phi'' + \frac{\phi'}{r} - \left(\alpha^2 + \frac{n^2}{r^2} \right) \phi \right] \right] \quad (7) \end{aligned}$$

$$\begin{aligned} (U - c) \left(\phi'' + \frac{\phi'}{r} - \frac{n^2}{r^2} \phi \right) + U' \phi' - (U - c) \frac{\alpha n \phi}{r^2} \\ = \frac{1}{i\alpha R_e} \left\{ \phi^{iv} + \frac{2}{r} \phi''' - \frac{1}{r^2} \phi'' (1 + 2n^2 + \alpha^2 r^2) + \frac{1}{r^3} (1 - \alpha^2 r^2 + 2n^2) \phi' \right. \\ \left. - \frac{1}{r^4} (4n^2 - n^4 - \alpha^2 n^2 r^2) - \frac{n\alpha}{r^2} \psi'' + \frac{3\alpha n}{r^3} \psi' - \left(\frac{4\alpha n}{r^4} - \frac{\alpha^3 n}{r^2} - \frac{\alpha n^3}{r^4} \right) \right\} \quad (8) \end{aligned}$$

The boundary conditions are,

$$\left. \begin{aligned} \psi, \phi, \psi', \phi' &= 0 \quad \text{at } r = r_o \\ \psi, \phi, \psi', \phi' &\rightarrow 0 \quad \text{as } r \rightarrow \infty \end{aligned} \right\} \quad (9)$$

Since the analysis here is carried out for a thick body, where Mangler's transformation (White, 1991) is valid and therefore a Blasius mean profile may be used. This constitutes an eigen value problem: a non-trivial solution is obtained for a given α and Re at particular values of phase speed(c) and growth rate ω . The least stable mode is one with the largest growth rate.

As described in (Govindarajan et. al. 2001) energy balance equation is obtained by taking the dot product of the linearised vector stability equations with the disturbance velocity vector and summing and averaging over one cycle in z. The averaged disturbance kinetic energy may be written as,

$$\left\langle \hat{E}(r, z, t) \right\rangle_z = \left\langle \frac{1}{2} [\hat{v}_z^2 + \hat{v}_r^2 + \hat{v}_\theta^2] \right\rangle_z = \mathcal{E}(r). \exp(2\omega_i t) \quad (10)$$

The final energy equation is in the form,

$$2\omega_i \mathcal{E}(r) = \nabla \cdot \mathbf{J}(r) + W_+(r) - W_-(r), \quad (11)$$

where energy flux $\mathbf{J}(r)$, energy production rate $W_+(r)$ and the dissipation $W_-(r)$ are given by,

$$\mathbf{J}(r) = \frac{1}{\text{Re}} \nabla \frac{\bar{U}^2}{2} + p \bar{\mathbf{U}} \quad (12)$$

$$W_+(r) = -\frac{1}{2} (v(r)_r v(r)_z^* + v(r)_r^* v(r)_z) \frac{dU}{dr} \quad (13)$$

$$\begin{aligned} W_-(r) = & \frac{1}{\text{Re}} \{ -\alpha^2 v(r)_z v(r)_z^* - \frac{n^2}{r^2} v(r)_z v(r)_z^* + v(r)'_z v(r)'_z - \alpha^2 v(r)_r v(r)_r^* + v(r)'_z v(r)'_z \\ & + \frac{1}{r^2} [v(r)_\theta v(r)_\theta^* - n^2 v(r)_r v(r)_r^* - in(v(r)'_r v_\theta \\ & + v(r)_r v(r)_\theta^*)] - \alpha^2 v(r)_\theta v_\theta^* + v(r)'_\theta v(r)'_\theta \\ & + \frac{1}{r^2} [v(r)_r v(r)_r^* - n^2 v(r)_\theta v(r)_\theta^* + in(v(r)'_r v(r)_\theta + v(r)_r v(r)_\theta^*)] \} \end{aligned} \quad (14)$$

where the superscript * denotes the complex conjugate. The total production and dissipation across the boundary layer are given by,

For an unstable perturbation Γ_+ would exceed Γ_- .

$$\Gamma_\pm \equiv \int_{r_o}^{\infty} W_\pm(r) dr \quad (15)$$

Method of solution

$$\begin{bmatrix} A_{11} & A_{12} \\ A_{21} & A_{22} \end{bmatrix} \begin{bmatrix} \psi \\ \phi \end{bmatrix} = \omega \begin{bmatrix} B_{11} & B_{12} \\ B_{21} & B_{22} \end{bmatrix} \begin{bmatrix} \psi \\ \phi \end{bmatrix} \quad (16)$$

Equations (6 and 7) with boundary conditions given by (8) are discretised using Chebychev polynomials and written in matrix form, where ω are the eigenvalues. The following grid stretching is used to allow greater clustering of grid for smaller γ near the wall. Here y_i are the

$$y(r)_i = \frac{(1 + y_i)\gamma}{1 + \frac{2\gamma}{l} - y_i} \quad (17)$$

Chebychev collocation points and l is the edge of the computational domain, which is specified to be about 5 times the boundary layer thickness. We use 81 collocation points, which gave an accuracy of 5 decimal places.

Results and discussions

Figure 1 shows neutral stability boundaries for different curvatures for an axisymmetric disturbance *i.e.* $n=0$. The critical Reynolds number increases with the transverse convex curvature. The minimum surface curvature used is $S_o=0.001$, Here S is defined as the inverse of the radial coordinate and the subscript o refers to the value at the body surface. The critical Reynolds number for this curvature is 200, which is close to the Orr-Sommerfeld solution for 2D boundary layers.

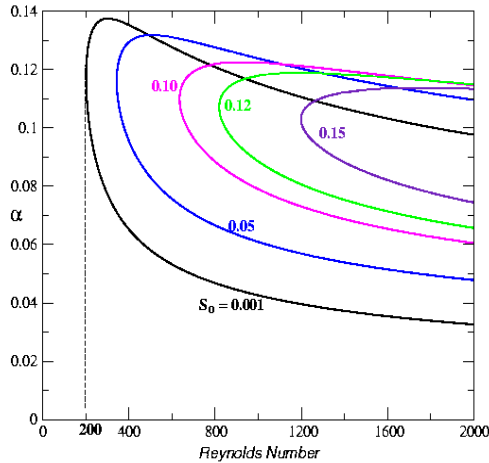


Fig.1 Neutral stability curves for different curvatures ($n = 0$)

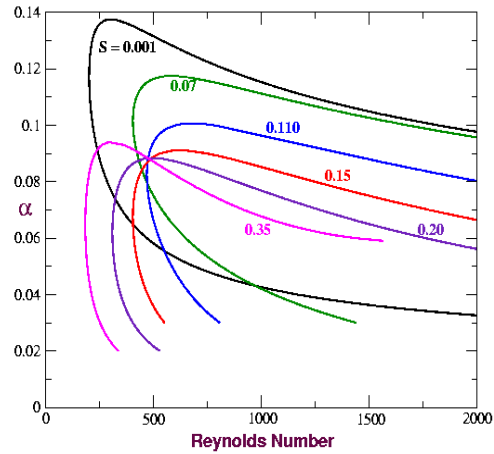


Fig 2. Neutral stability curves for different curvatures ($n=1$)

In the case of mode $n=1$ (fig.2) , where a single wave encircles the body, the critical Reynolds number increases with curvatures at small curvatures. After reaching a maximum value at some curvature it starts decreasing. This means that there is a critical curvature for which the first ($n=1$) non-axisymmetric mode is most stable.

For all higher modes ($n=2,3,\dots$) the critical Reynolds number increases with curvature. (Fig .3). The range of unstable frequency also becomes narrower as the curvature increases. Modes

3 and above never become dominant for the curvatures considered. So it is sufficient to study only the first three modes.

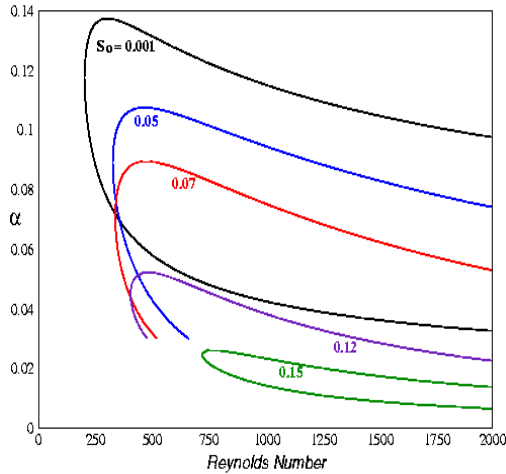


Fig. 3 Neutral stability curves for different curvatures ($n=2$)

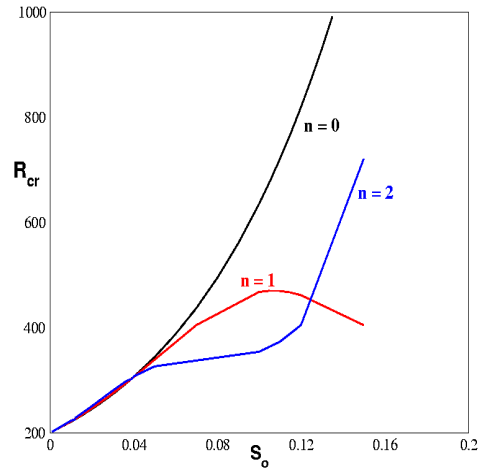


Fig. 4 Surface curvature Vs critical Reynolds number for different modes

The critical Reynolds number is plotted against surface curvature is plotted for different modes in fig 4. It is clear that the axisymmetric mode is dominant for surface curvatures less than 0.04 and the second mode ($n=2$) is least stable when curvature is between 0.04 and 0.125. For any higher curvatures the first mode is the most unstable one. For higher modes ($n=3,4,..$) the critical Reynolds number increases with curvature.

Figures 5,6 and 7 show the distribution across the boundary layer of the production and dissipation of disturbance kinetic energy for these different modes. The curvature chosen is $S_0=0.025$ and Reynolds number is 260. As expected the productions peak in the respective critical layers of the modes, while the dissipation is maximum at the wall. In this case mode 0 is unstable, while $n=1$ and $n=2$ are stable. It is noteworthy, however that there is a significant overlap of the production zones of these. This indicates a possibility of early non-linear interaction between the modes. Mode 2 shows a second dissipation peak close to the maximum in production. These issues along with the quantitative of local disturbance kinetic energy for a range of curvatures will be presented at the conference.

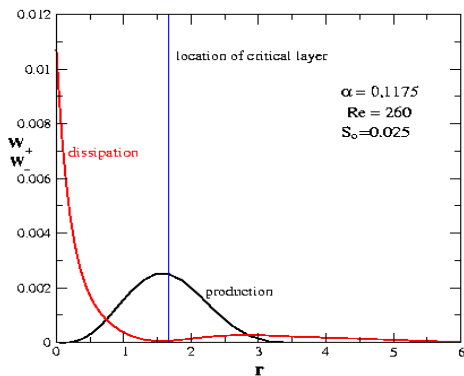


Fig 5. production and dissipation at mode $n=0$

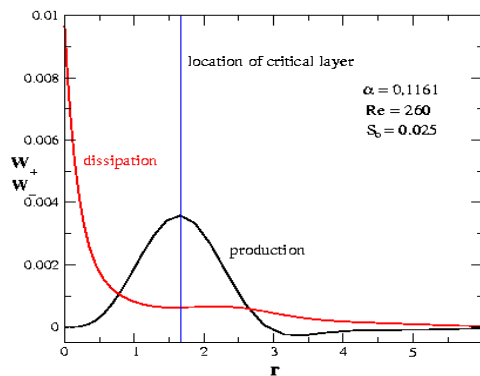


Fig 6. Production and dissipation of mode $n=1$

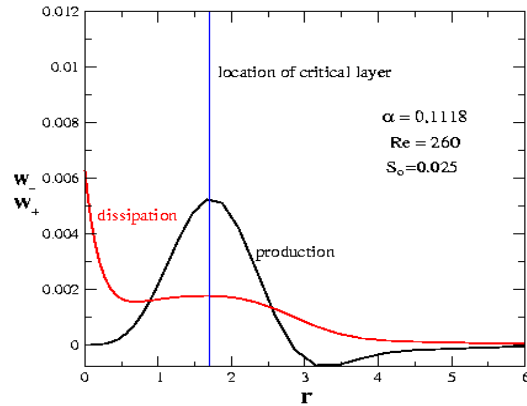


Fig 7. Production and dissipation of mode $n=2$

Conclusions

It is demonstrated that the transverse curvature has a direct effect on the stability of an axisymmetric boundary layer. In these flows the non-axisymmetric modes ($n=1$ and 2) play a dominant role at higher curvatures.

REFERENCES

- [1] Fox, J. A., Lessen, M. & Bhat, W. V., 1968, Experimental investigation of the stability of Hagen-Poiseuille flow, *Phys. Fluids* 11,1-4.
- [2] Leite, R. J., 1959, An experimental investigation of the stability of Poiseuille flow, *J. Fluid. Mech.*, 5,81
- [3] Lessen, M., Saddler, S. G. and Liu, T. Y., 1968, Stability of pipe-Poiseuille flow, *Phys. Fluids*, 11, 1404-1409.
- [4] Rao., G.,N.,V., 1967, Mechanics of transition in axisymmetric boundary layer on a circular cylinder, *ZAMP*, 25,63-75.
- [5] Squire, H. B., 1933, On the stability of three dimensional disturbances of viscous flow between parallel flows, *Proc. Roy. Soc. A.*,142, 621-628.
- [6] Govindarajn, R, V.S.L'vov and I. Procaccia, 2001, Retardation of the onset of turbulence by minor viscosity contrasts, *Phy. Rev. Letters*. to be appeared